VibID: User Identification through Bio-Vibrometry

Lin Yang[†], Wei Wang[‡†], Qian Zhang[†]
[†]Hong Kong University of Science and Technology,
[‡]School of Electronic Information and Communications, Huazhong University of Science and Technology

***Abstract*— User identification is an essential problem for security protection and data privacy preservation of wearable devices. With proper user identification, wearable devices can adopt personalized settings for different users, automatically label the corresponding data to protect user privacy, and help prevent illegal user spoofing attacks. Current user identification solutions proposed for wearable devices either rely on dedicated devices with high cost or require user intervention which is not convenient. In this work, we leverage the bio-vibrometry to enable a novel user identification solution for wearable devices in small-scale scenarios, *e.g.*, household scenario. Unlike existing user identification solutions, our system only uses the low-cost sensors that are already available for most wearable devices. The key idea is that, when human body is exposed to a vibration excitation, the vibration response reflects the physical characteristics of user, *i.e.*, the *mass*, *stiffness* and *damping*. Meanwhile, due to users' biological diversity, such physical characteristics of different users are quite distinctive. Therefore, we can leverage the discrepancy in users' vibration responses as an identifier. Based on this idea, we propose VibID, which only uses a low-cost vibration motor and accelerometer to generate an unobtrusive vibration to users' arms and capture the corresponding responses. By examining the vibration patterns at different frequencies, VibID builds an ensemble machine learning model to recognize who is using the device. Extensive experiments are conducted on human subjects to demonstrate that our system is reliable in small-scale scenarios and robust to various confounding factors, *e.g.*, arm position, muscle state, user mobility and wearing location. We also show that, in an uncontrolled scenario of 8 users, our system can still ensure a identification accuracy above 91%.**

I. Introduction

Nowadays we are witnessing the fast development of wearable devices. With the ability of providing unobtrusive and continuous services, wearable devices have not only brought about great convenience, they have penetrated into every part of our daily life. We may use a wearable device to track daily activity levels (*e.g.*, Fitbit Charge [1]), interact with other smart devices (*e.g.*, Apple watch [2]) or monitor the state of our health (*e.g.*, Google's smart contact lens for diabetes [3]).

In some scenarios, it is quite common that we share wearable devices with others. For example, in a household scenario, a group of family members may share a smart sphygmomanometer, or in a medical center, a wearable heart rate monitor is assigned on demand to several patients with chronic cardiac disease. In these scenarios, recognizing *who is using this device* becomes an essential problem for protecting data privacy and security. For activity-tracking devices, user identification can help the device to load corresponding profile for each user, and automatically label the user's data; For interaction-augmenting devices, *e.g.*, Apple watch or Google glass, knowing who is using this device enables better content access control and privilege authentication; For health-monitoring devices, user identification can help the improvement of data security and privacy protection.

However, wearable devices have many limitations as far as size, cost, energy and computation power, which makes traditional user identification methods cannot fit well in their target scenarios: a conventional PIN code cannot be used prevalently as the size constraint of most wearable devices leads to a lack of user-friendly input methods. Although the camera and fingerprint reader offer a good user experience, their high cost and computation requirements hinder their wider-adoption on wearable devices. Recent research in this area has mainly focused on either biometrics or user behavior modeling. Researchers have validated the possibility of using the human body capacitive [4], bio-impedance [5] and walking gait [6] to extract unique patterns to identify users. However, these works either require a dedicated sensor, *e.g.*, a bio-impedance sensor, or need user intervention, for example, gait only works when the user is walking. On the other hand, some works try to distinguish users by modeling their usage behavior, *e.g.*, data stream on mobile phone [7], touch behavior and holding posture of device [8, 9]. However, accurate behavior modeling places a challenging requirement on computation power and energy, which are scarce resources for wearable devices.

In our vision, a user identification method should meet the following requirements to be truly pervasive: (1) instead of requiring an additional and expensive devices, we should leverage existing low-cost devices/sensors available on most wearable devices. (2) The whole procedure of user identification should be unobtrusive and does not require any user intervention; (3) The system should be robust to user spoofing attacks. (4) Good performance in various scenarios.

To satisfy these requirements, we propose VibID – a low-cost and reliable user identification system for wearable devices using bio-vibrometry. The key idea of VibID is that, when a mechanical vibration is applied on user's body, *e.g.*, forearm, the excitation will cause the body tissues to vibrate, which is termed as "response". According to the theory of vibration, the pattern of such vibration response not only depends on the excitation but also on the physical characteristics of users, *i.e.*, the *mass*, *stiffness* and *damping*. Besides, due the biological diversity of users, such characteristics of different users diversify, which results in the significant discrepancies among users' vibration responses. This implies that, we can apply same excitation to different users and leverage the

978-1-5090-0802-5/16/$31.00 ©2016 IEEE

discrepancies in their vibration responses to recognize users.

Inspired by this idea, we design VibID to be a wristband-like device consisting of a haptic vibration motor and an accelerometer, both of which are low-cost devices available on most wearable devices. By applying a specially-designed excitation on users' forearms, we can capture the corresponding vibration responses and extract various temporal and spectral features from these responses. Then, such features can be used to build a user identification classifier via an ensemble machine learning algorithm. Our system is not intended to be a strict security measurement. Instead, we target our system as a convenience to help wearable devices recognize users in small-scale scenarios where the set of different possible users is small and the consequences of a mis-classification are benign. For example, recognizing which family member is using this device in a household scenario.

To realize such system, we need to address several challenges. First, it is not clear how to use the vibration response of the human body to distinguish users. To this end, we formulate the vibration model and make several insights on the relationship between vibration responses and physical characteristics of human body. Moreover, even though there exists a biological diversity in users, such difference can be quite small among some users, which makes the discrepancies among users hard to be observed. To combat this challenge, we carefully design our excitation pattern and leverage the effect of resonance to magnify the difference. Third, as human body is a complex system, there are various confounding factors that can affect our system. We comprehensively explore the impact of these factors by extensive experiments on volunteers.

Our contributions in this work lay in the following aspects:

- As far as we know, we are the first to explore the possibility of using bio-vibrometry to enable use identification for wearable devices. We have demonstrated that the discrepancies which exist in users' responses are sufficient for user identification in small scale, *e.g.*, household scenario.
- We design VibID, which leverage vibration responses to enable user identification for wearable devices. Its implementation only requires a low-cost vibration motor and accelerometer, both of which are low-cost and common components for most wearable devices.
- We comprehensively evaluate the performance of our system under different scenarios. The result indicates the VibID is robust in different scenarios with the presence of various confounding factors. Also, our experiment in uncontrolled scenario with 8 users shows that VibID can ensure a good identification accuracy above 91%.

The rest of the paper is organized as follows. We briefly introduce the theory of vibration and investigate the feasibility of using vibration to distinguish users in section II. The System design and detailed implementation are discussed in section III and IV, respectively. In section V, we present the evaluation result of our system. The discussion and related work are provided in section V and VII, followed by the conclusion in section VIII.

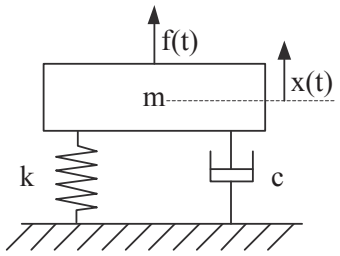

Fig. 1. Single DoF system.

II. Feasibility of Bio-Vibrometry

In this section, we start with a brief review of vibration theory, which lays the foundation of our system. Then, we discuss how to use vibration to identify users on wearable device and validate its feasibility through experiments.

A. Basic Vibration Theory

Vibration is one of the most common mechanical phenomenons in our physical world, in which oscillations occurs about an equilibrium point [10]. To study the vibration of a mechanical system, we need to first introduce the dynamic properties of mechanical systems: the *mass*, *stiffness* and *damping*, which are responsible respectively for inertia, elastic and dissipative forces. As the vibration of a mechanical system is the result of all of these features interacting with each other, perfect modeling of vibration can be a very complex problem, if not impossible. However, in most cases, we can break the all system into several sample elements and start with a single degree-of-freedom (SDoF) model, which can be explicitly modeled and easily analyzed. After that, if these SDoF models are properly combined, a more complex and accurate model, *i.e.*, multiple degree-of-freedom (MDof), can be learned.

Figure 1 presents the dynamic properties of a SDoF system. In this system, the inertia is represented by an infinitely rigid constant mass m, elasticity is defined as an ideal massless spring of constant stiffness k, and the damping is represented by a viscous damper with damping coefficient c.

When applied with an external excitation force $f(t)$, the displacement $x(t)$ of the system satisfies the following equation:

$$m\ddot{x}(t) + c\dot{x}(t) + kx(t) = f(t), \tag{1}$$

where $f(t)$ and $x(t)$ are the time-dependent excitation force applied to this system and corresponding displacement response, while the $\dot{x}(t)$ and $\ddot{x}(t)$ is the first and second derivative of $x(t)$, *i.e.*, the speed and acceleration.

Free Vibration corresponds to the scenario where $f(t) = 0$. In this case, equation (1) has a general solution as: $x(t) = Xe^{st}$, where s is the Laplace variable to be determined. Substituting this general solution into equation (1) leads to:

$$(ms^2 + cs + k)Xe^{st} = 0, \tag{2}$$

yielding two roots s_1 and s_2:

$$s_{1,2} = -\frac{c}{2m} \pm \sqrt{\left(\frac{c}{2m}\right)^2 - \frac{k}{m}}, \tag{3}$$

Notice that depending on the value of $\sqrt{\left(\frac{c}{2m}\right)^2 - \frac{k}{m}}$, the roots can further fall into three cases:

- $\left(\frac{c}{2m}\right)^2 > \frac{k}{m}$: over-damped system, where both roots are real;
- $\left(\frac{c}{2m}\right)^2 < \frac{k}{m}$: under-damped system, where two roots are complex conjugate;
- $\left(\frac{c}{2m}\right)^2 = \frac{k}{m}$: critically-damped system with two equal roots;

Therefore, the solution of equation (1) when $f(t) = 0$ is:

$$x(t) = C_1 e^{s_1 t} + C_2 e^{s_2 t}, \tag{4}$$

where $C_{1,2}$ are constant determined by the initial condition.

By defining a critical damping coefficient c_c and damping ratio ξ as follows:

$$c_c = 2\sqrt{km} = 2mw_n \tag{5}$$

$$\xi = \frac{c}{c_c}, \tag{6}$$

we can further derive detailed solution for under-damped system as following:

$$x_{ud}(t) = e^{-\xi w_n t}\Big[x(0)\cos\left(w_n t\sqrt{1-\xi^2}\right) + \frac{\dot{x}(0) + \xi w_n x(0)}{w_n\sqrt{1-\xi^2}}\sin\left(w_n t\sqrt{1-\xi^2}\right)\Big], \tag{7}$$

where $w_n = \sqrt{\frac{k}{m}}$ is the undamped natural frequency, $x(0)$ and $\dot{x}(0)$ are the displacement and velocity at initial state, respectively.

In **Forced Vibration**, the external force is assumed to be: $f(t) = Fe^{iwt}$, where F and w are the amplitude and frequency of the harmonic excitation. In this case, the particular solution of equation (1) is given by:

$$\begin{aligned} x_F(t) &= \frac{F}{\sqrt{(k-w^2m)^2 + (wc)^2}} e^{i(wt+\theta)} \\ &= \frac{F}{k}\frac{1}{\sqrt{(1-\beta^2)^2 + (2\xi\beta)^2}} e^{i(wt+\theta)}, \end{aligned} \tag{8}$$

where $\beta = \frac{w}{w_n}$ is the ratio of excitation frequency and undamped natural frequency of system, and θ is the phase delay and defined by: $\tan\theta = \frac{-wc}{k-w^2m}$.

The completed response of a mechanical system under external force $f(t)$ is given by the sum of free vibration and forced vibration. As most vibrations in our daily life are under-damped systems, we can write the response as the summation of equation (7) and equation (8):

$$resp(t) = x_{ud}(t) + x_F(t) \tag{9}$$

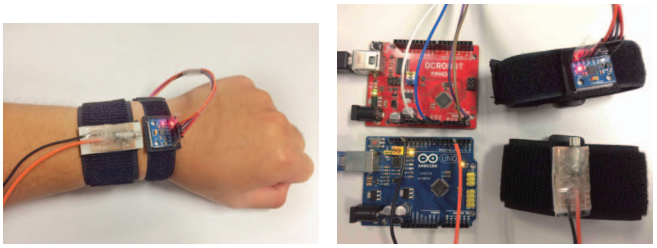

(a) Installation of prototype. (b) Components in prototype.

Fig. 3. Data collection prototype.

B. User Identification through Bio-Vibrometry

According to above theoretic analysis of system's response in forced vibration, we can make several observations:

- The vibration frequency of response is same as the excitation force.
- Given the same excitation, the amplitude of partial response contributed by the forced vibration, $x_F(t)$, only depends on system's mass m, stiffness k and damping c.
- The response caused by under-damped vibration is more complicated as it depends on not only system's characteristics, but also the initial state.
- Theoretically speaking, the effect of under-damped vibration always exists. In reality, however, it is only noticeable for short period at the beginning, as its power decays quickly. The short initial period with free vibration is termed as "transient state", while the remaining period where forced vibration dominates is called "steady state".

We also notice there exists a diversity in users' heights, weights and body mass index (BMI), which are directly related to the mass, stiffness and damping of human body. Even users with similar weight, height and BMI, their underlying body composition, *e.g.*, the ratio of muscle and fat, or even the bone size, can be quite different [11].

Inspired by these observations, we form the key idea of our system: we can apply a specially-designed excitation to user's body, *e.g.*, forearm. As the body compositions of different users diversify, their mass, stiffness and damping are different, which leads to different responses to same excitation. Therefore, we can use this discrepancy as biometric to distinguish users.

C. Feasibility

To validate the feasibility, we designed a data collection prototype as shown in Figure 3. This prototype consists of a haptic vibration motor [12] and an InvenSense MPU-6050 sensor with a three-axis accelerometer [13]. The vibration motor is driven by an Arduino development board to generate a stepped sine-sweep excitation, in which the frequency and amplitude of generated vibration increases with time. As the natural frequencies of human arm-hand system range from 5 Hz to 1 KHz [14], we choose an excitation stepping from 23 Hz to 133 Hz, which allows us to observe vibration response spanning multiple natural frequencies (More details

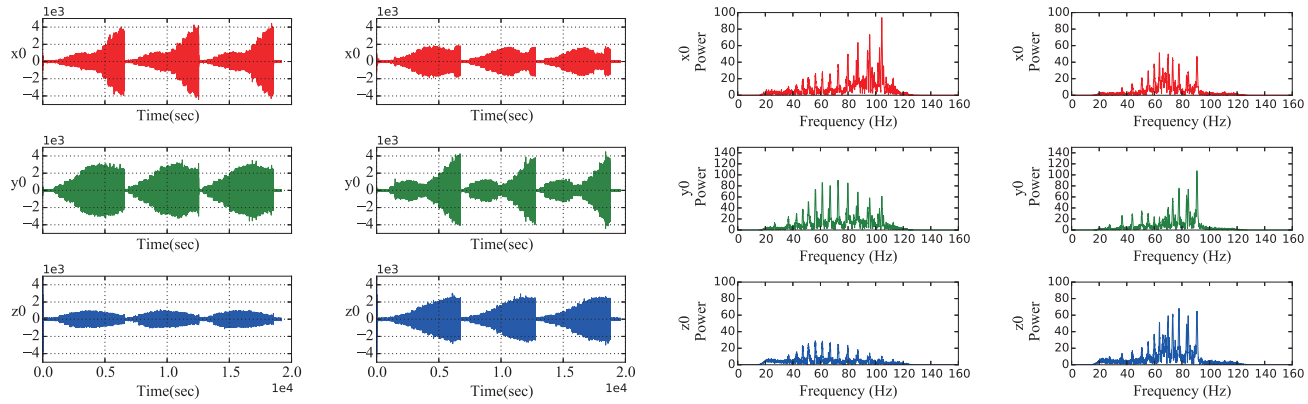

(a) Temporal Response of user 1 (b) Temporal Response of user 2 (c) FFT of user 1's response (d) FFT of user 2's Response

Fig. 2. Responses of two users.

of excitation design are discussed in section III-A). We ask 8 volunteers to wear this prototype on their wrist, while applying the stepped sine-sweep excitation to users, we capture their vibration responses via an accelerometer with sampling frequency of 320 Hz.

Figure 2(a) and 2(b) show an example of responses from two different users. Note there are three separated responses in each axis. From these figures, we can make some immediate observations: first, the three responses of same user is consistent. Second, there exists a significant discrepancy between responses of two users. To further demonstrate the difference, we plot the power spectrum of responses of these two users in Figure 2(c) and 2(d), we observe that, for X axis of accelerometer, most power of user 1 concentrate on high frequencies (90 100 Hz), while power peak of user 2 appears around 70 Hz. Similar observations can be found in Y and Z axis.

These results indicate that we can leverage the unique pattern of users' response as an identifier and validates our idea. In next section, we discuss how to build a user identification system based on this idea.

III. System Design

In this work, we do not aim to exactly estimate the characteristics of human body from their vibration responses. Such analysis requires strictly-controlled experiment setting and high computation power. Instead, we are interested in utilizing the discrepancy in users' vibration responses caused by their' biological diversity as user identifier. Figure 4 show the architecture of our system.

Generally, this system can break into two major parts:

- **Vibration response collection**: This part is responsible for generating specially-designed excitation and capture corresponding vibration responses. It is designed to be a wristband-like device as shown in Figure 3, which consists of a haptic vibration motor and an InvenSense MPU-6050 accelerometer with a maximal sampling frequency of 320 Hz. The major challenge of this part lies in the fact that the difference between some users can be quite small and such minor difference can be hard to be observed in users' vibration responses. To alleviate this problem, we need to carefully design the excitation to magnify the discrepancy between users. Section III-A discusses how we drive the vibration motor to generate such excitation pattern in detail.
- **User identification**: After capturing users' vibration responses, we first apply a bandpass filter to eliminate the interference of environment and user mobility (details in section III-B). Then, we can divide each response data into segments of different vibration frequencies, and temporal features are extracted from each segment. These features are used to train a user identification model via random forest and used for further real-time identification (Section III-C).

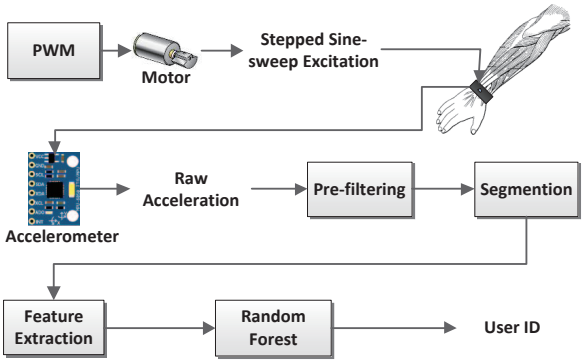

Fig. 4. System overview.

A. Design of Excitation

According to the discussion in section II, we have already known that the diversity of users' biological composition results in differences in their vibration responses. To leverage this discrepancy to distinguish users, an intuitive solution is to randomly pick an excitation and examine users' vibration

responses. However, this solution is not practical, the major concern comes from the fact that such discrepancy may be not significant enough to be observed. For example, the damping ratio ξ of human arm fluctuates around 0.5 with a small deviation [14]. In most cases, such small variation in ξ can be hard to be observed from users' vibration responses. To alleviate this problem, we need to magnify the differences in users' vibration response.

To find the solution, we need take a close look at the response caused by forced vibration, *i.e.*, equation (8). From this equation, we can make some further observations: (1). when $\beta \approx 1$ and $\xi \approx 0$, *i.e.*, the excitation frequency is close to the natural frequency and the damping ratio is small, the denominator approximates zero. Thus the amplitude of response goes to "infinity". This situation is termed as the *resonance*. (2). In the case of resonance, as β approximate 1, the denominator is fully dominated by ξ. Therefore, the amplitude of response is totally determined by the value of ξ and the effect of ξ can be clearly observed. Figure 6 illustrates this observation by comparing the responses of systems with different damping ratios near resonance. We can observe that when ξ is small, which is true in our case, the difference is significant. Therefore, if we can excite users' arm at their natural frequency, the discrepancy in users' vibration response can be more obvious and thus improve the quality of user identification.

However, according to previous studies [14, 15], the natural frequencies of human arm range from several Hertz to hundreds of Hertz. As a result, instead of using excitation of single frequency, we choose to use a "frequency-sweeping" excitation whose vibration frequency slowly steps from low frequencies to high frequencies. Obviously, the more frequencies the excitation spans, the more details can observed from responses, but also longer excitation time requires.

To generate such excitation, we use an Eccentric Rotating Mass (ERM) vibration motor, which is commonly used in mobile phones and wearable devices for notification and haptic feedback. Figure 5 shows a sample ERM vibration motor, where a non-symmetric mass is attached to the shaft of a DC motor. When the motor rotates, the centripetal force of the eccentric mass is asymmetric, resulting in a vibration. The centripetal force F generated by eccentric mass is given by:

$$F = mrw^2 \sin(wt) \tag{10}$$

where m is the eccentric mass attached to the shaft, r is the distance from the motor shaft to the center of the eccentric mass, and w is the rotating angular velocity. We observe that the frequency and amplitude of generated excitation force are both determined by the angular velocity w, which is directly proportional to the input DC power voltage. As a result, we can control the generated excitation by manipulating the input voltage to ERM vibration motor.

In our system, we control the vibration motor with Pulse Width Modulation (PWM), which is a way of digitally encoding analog signal levels [16]. The key idea of PWM is to simulate an analogy DC voltage input by modulating the duty cycle of a high-resolution square pulse. For example, to output a voltage of 3V with a 5V DC power, we can set the duty cycle of PWM to be 60%. Note that, due to the principle of ERM vibration motor, we cannot control its frequency and amplitude separately. Thus, if we increase the vibration frequency, its amplitude also grows. Figure 7 shows an example of generated excitation by using PWM on ERM vibration motor.

Also, as mentioned in section II, the free vibration dominates a short period of time at the beginning of vibration response. As the free vibration depends on not only users' characteristics, but also the initial state, it is hard to analyze its patterns. Therefore, during the procedure of frequency sweeping, the vibration motor will vibrate at each frequency for t seconds. The value of t need to be large enough to ensure that the effect of free vibration is diminished and the system enters the steady state.

B. Pre-filtering

In the real application scenario of VibID, it is inevitable for our system to perform user identification with various interferences. The most significant one derives from users' mobility, *e.g.*, user movement or hand gesture. Figure 8 shows the power spectrum of accelerometer reading when a user is walking while texting messages on his phone. It is obvious that the power of user mobility concentrates at frequencies lower than 5 Hz. Many other studies also confirm this fact [17, 18]. As our excitation starts from 23 Hz, we can easily eliminate the interference by using a Butterworth bandpass filter [19], with a cutting-off frequency from 15 Hz to 135 Hz.

C. User Identification

Since the information of users' characteristics are encoded in the amplitude of their vibration response, especially near the natural frequencies, we need to examine the vibration responses at different frequencies. To this end, we first divide response data into multiple segments, each of which only contains a vibration of a constant frequency. This is easily done as response frequency is same as the excitation frequency, and the duration of each excitation frequency is controlled by our system. For each segment, temporal features shown in Table I are extracted for all three axes.

TABLE I
FEATURES

Feature	Meaning
freq	vibration frequency of segment
min	minimum of segment
max	maximum of segment
25p	the 25th percentiles of segment
50p	the 50th percentiles of segment
75p	the 75th percentiles of segment
std	the standard deviation of segment

With these features, we build a user identification model based on *Random Forest*, which is a is an ensemble machine learning model based on Decision Tree [20].

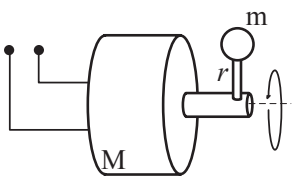

Fig. 5. ERM vibration motor.

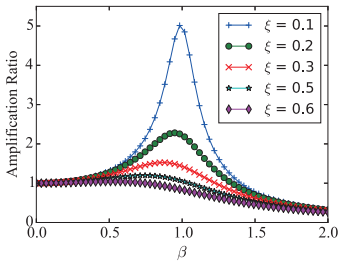

Fig. 6. Amplification ratio.

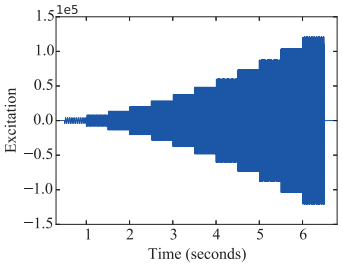

Fig. 7. Stepped sine-sweep excitation.

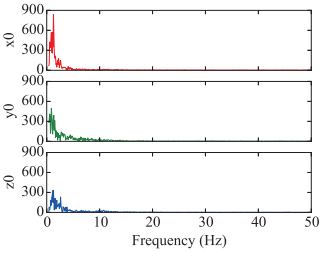

Fig. 8. FFT of user mobility.

To address the overfitting problem of Decision Tree, The random forest model introduces the bootstrap aggregating technique in the training of model. The key idea of random forest is that, given a training set $X = x_1, ..., x_n$ with corresponding labels $Y = y_1, ..., y_n$, the model randomly selects m samples from training set with replacement. Also, a similar sampling scheme is applied on feature selection. By repeating this sampling process N times, it will generate N training sets. Then, a decision tree is trained from each training set. After that, the predication for a test data can be made by taking the majority vote from all the N individual decision trees. Although a single decision tree can be highly sensitive to the noise in the training set, the average of trees is not. As a result, such bootstrapping procedure can decreases the variance of the model without increases the bias, which lead to a better model performance.

In the application scenario of VibID, when a user wears our wristband for the first time, a short initial phase is needed, in which 10 excitations are applied on user's arm and corresponding responses are collected for the training of classifier. After that, each time the user wears on the wrist band, an excitation is automatically applied and corresponding response is used to identify user.

IV. Implementation

We implement VibID as a wristband-like device as shown in Figure 3.

In this prototype, we use an Arduino UNO development board to control an InvenSence MPU6050 accelerometer and a haptic vibration motor with maximal 3.3V input voltage. We have developed an application to control the input power voltage of vibration motor via PWM. The generated vibration frequency spans from 23 Hz to 133 Hz. The vibration duration at each frequency is set to be 1.4 seconds, which is longer than we really need for the purpose of experiment. Table II shows the measured vibration generated by our prototype.

Since the highest frequency of excitation we supported is about 133 Hz, we sample the accelerometer at 320 Hz, which is sufficient to observe all the responses at given excitation frequencies.

For the user identification, the data per-processing and bandpass filtering are implemented with Python 2.7, while the random forest classifier is built based on scikit-learn package [21].

TABLE II
Specification of Vibration Motor

Voltage (V)	Vibration Frequency (Hz)	Vibration Amplitude (G)
0.59	23.5	0.29
0.98	44.1	0.36
1.37	61.5	0.57
1.76	80.4	0.68
2.16	102.2	1.03
2.54	123.1	1.42
2.95	133.4	1.94

V. Performance Evaluation

To evaluate our system, we conduct user identification test with 8 volunteers (5 males and 3 females). Each volunteer is asked to wear the VibID wristband prototype on their forearms and the corresponding response data are collected and offload to a laptop for further experiments under different settings.

First, we investigate the impact of the confounding factors to our system, which includes: (a) excitation configurations, such as: the frequency bandwidth of excitation and vibration duration of each frequency, (b) user states, including user's arm posture, muscle state or mobility, and (c) usage issues, *e.g.*, the wearing location of wristband. To investigate the impact of a confounding factor, we carefully control the experiment setting by changing the value of this confounding factor while retain the others unchanged, and collect 15 records from each volunteer at each experiment setting ($8 \times 15 = 120$ records at each setting). Then, we use these data to investigate how this confounding factors affect the performance of our system.

After that, we perform an overall evaluation in an uncontrolled scenario. In this experiment, instead of carefully controlling the confounding factors, we ask each volunteer to use VibID as she/he wants and collect 120 response data under various uncontrolled scenarios. Then, all of these collected data ($8 \times 120 = 960$ records) are used to evaluate the performance of our system via 10-fold cross validation.

Throughout the whole evaluation, we use two metrics to evaluate the performance:

- **Precision**, which is a measure of exactness for classifiers, *i.e.*, the percentage of tuples labeled as positive are actually such. In binary classification, precision is defined as $P = \frac{TP}{TP+FP}$, where TP and FP are the count of *true positive* and *false positive*. For multi-class problems,

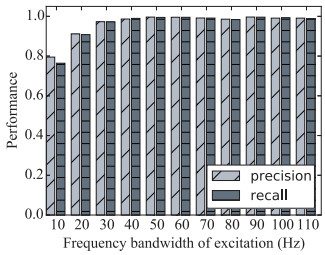

Fig. 9. Impact of excitation bandwidth.

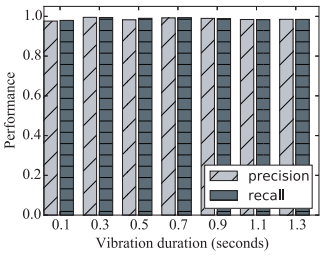

Fig. 10. Impact of vibration duration.

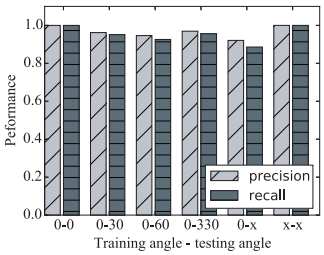

Fig. 11. Impact of arm posture.

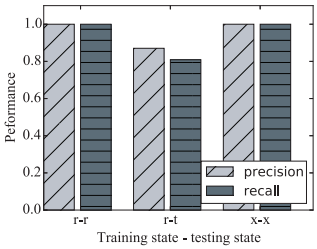

Fig. 12. Impact of muscle state.

it can be generalized as follows:

$$P = \frac{\sum_{i=1}^{l} \frac{TP_i}{TP_i+FP_i}}{l}, \tag{11}$$

where l is the number of classes, TP_i and FP_i are the *true positive* and *false positive* of i-th class, respectively.

- **Recall** measures the completeness of a classifier, which is defined as the percentage of positive tuples are predicted as positive ones, *i.e.*, $R = \frac{TP}{TP+FN}$ in binary classification. Again, for multi-class problems, it can be extended as follows:

$$R = \frac{\sum_{i=1}^{l} \frac{TP_i}{TP_i+FN_i}}{l}, \tag{12}$$

where l is the number of classes, TP_i and FN_i are the *true positive* and *false negative* of i-th class, respectively.

Note that above generalizations of precision and recall are referred as the "macro-averaging", which gives equal weights to all classes when computing the averaged precision and recall. However, there is another generalization approach named "micro-averaging", in which each tuple makes equal contribution to the overall metric and thus big classes with more tuples are preferred when averaging [22]. As the identification of each user is equally-important in our scenario, we adopt the macro-averaging approach.

Subsection V-A, V-B and V-C evaluate the impact of excitation configuration, user state and usage issues, respectively. The results for these experiments demonstrate our system is robust to these confounding factors. Also, the overall test in section V-D shows that VibID can archive a high identification performance (average precision=0.98, recall=0.96) in an uncontrolled scenario of 8 users.

A. Excitation Configuration

The configuration of excitation, *i.e.*, its frequency bandwidth and vibration duration of each frequency, plays a vital role in our system. A wider frequency band of excitation can explore more information from different frequencies and a longer vibration duration time can alleviate the interference of transient-state vibration, but both of them require longer excitation time, which will degrade user's experience. To find the balance between performance and usability, we study the choices of these configurations affect our system in this section.

1) Frequency Bandwidth: As discussed in section III-A, when the excitation frequency is near the natural frequency of users' arms, the resonance effect can magnify the differences in users' characteristics, *i.e.*, the damping ratio ξ. Therefore, a wide frequency bandwidth of excitation which can help exhibit more patterns near the natural frequencies, but it also requires a longer excitation duration, which degrades the user experience of our system.

To find the optimal frequency bandwidth of excitation, we collect users' response data under various excitations of different frequency bandwidth. For this test, the vibration at each frequency is empirically set to 1.4 seconds, which is longer than needed according to our experience. Then, we use these data to perform use identification and compare the system performance via 10-fold cross validation. Note that, since the lowest excitation frequency of our system is 23 Hz, a frequency bandwidth of 10 Hz includes frequencies from 23 Hz to 33 Hz, and so on.

According to Figure 9, both precision and recall generally increase as the frequency bandwidth enlarges, as more response patterns at different frequencies can be explored. Meanwhile, we observe a diminishing effect of marginal utility, *i.e.*, when the frequency bandwidth of excitation is larger than 40 Hz, the gain of wider excitation bandwidth diminishes. This may result from the fact that a 40-hertz excitation band stepping from 23 to 63 Hz has already included the natural frequencies of most human arms.

Therefore, as a compromise between performance and usability, we set the frequency bandwidth of excitation to be 40 Hz in our system and used this setting for the remaining experiments.

2) Vibration Duration: Another important design concern of excitation is the vibration duration of each frequency. As the free vibration and forced vibration both coexist in users' responses, a longer vibration duration can ensure the system enter the steady state in which the interference of free vibration is negligible. However, a longer vibration degrades user' experience.

To find the optimal value of vibration duration, we first collect users' response data by using different vibration duration at each vibration frequency. Then, we compute the precision and recall of VibID with users' data collected under different vibration durations and report in Figure 10. Surprisingly, we find there are not much difference between these settings.

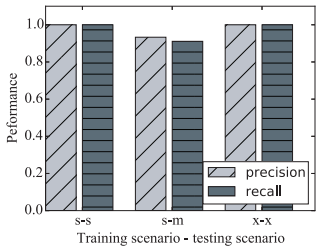

Fig. 13. Impact of user mobility.

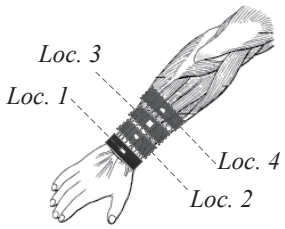

Fig. 14. Wearing locations on user's arm.

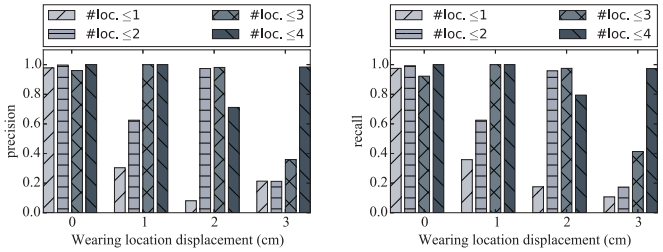

(a) Precision (b) Recall

Fig. 15. Impact of wearing location.

To further investigate the reason behind this result, we have examined all the users' response data and observed that the interference of transient state is quite minor in our system. Figure 16 shows an example case, where the upper figure is a user's response data along Y axis, while the lower one is the close-up of the response in the red-dot-line box. We highlight the transient state in the close-up and find that this period only lasts less than 0.07 seconds. This is due to the fact that our excitation is quite small with respect to the mass of arm, thus the effect of free vibration is insignificant. As a result, a small vibration duration would be sufficient for our system. Consider the controlling granularity of vibration motor and other hardware constraints, we set the vibration duration to 0.5 seconds and use this setting in the remaining experiments.

B. User State

In our vision, a reliable user identification system should be robust to various confounding environments. In this section, we evaluate how the confounding factors from user side affect our system's performance, including: arm position, muscle state and user mobility.

1) Arm Position: By designing VibID to be a wristband-like device, the user identification of our system can easily be triggered by a specific user motion, *e.g.*, raise the forearm as we did when trying to read the time from the watch. However, in real application, we can image that our system need to perform user identification under different arm/hand position, because the arm positions of this motion can be different each time.

To examine the impact of arm position, we ask volunteers to place their arm in different positions of various angles with respect to the ground. For example, 0° indicates the arm is parallel to the ground, while 30° means the arm rotates 30 degree clockwise from the position in 0°. For each position, we collect 15 responses from each user, so there will be 120 responses (15×8 users) under each position. Then, to simulate various application scenarios, we train our system with responses collected from a specific angle, *e.g.*, 0°, but test with responses from different angles.

Figure 11 shows the result of this experiment. Note that the x axis is labeled in the format of "training angle - testing angle". For example, "0 - 30" indicates that we train our system with data collected at 0° arm angle but test with data from 30°, and "0 - x" means the classifier is initialized with 0° data, but test with responses collected under different arm positions.

From this figure, we notice there is a small decrease in system performance if we train and test our system with data collected from different arm positions. The reason, we suspect, is due to a slight drift of underlying tissues when the arm position changes, especially for connecting tissues, such as fat and synovial membranes. However, such degradation is quite minor, in most case, our system still can achieve a precision above 91.2% and a recall larger than 89.7%, which is sufficient for our system.

2) Muscle State: We also investigate whether the muscle states of users' arms affect our system. To this end, we have collected two data set: First, we ask volunteers to squeeze their hand hardly during the experiments in order to collect their response data when their arms are in tense state. Also, we collect another set of data when users' arm is in relaxed state for comparison. By training and testing our system with users' response data collected from different muscle states, we explore the effect of muscle state and present the result in Figure 12. Again, for the simplicity, we name the experiment setting labeled at X axis as previous experiment similarly, where "r-t" means the system is trained with data from relaxed muscle but tested by data collected when users' arms are in tense state, and "x-x" stands for using both data from relaxed/tense muscle states to train and test our system.

According this figure, we can see an obvious performance attenuation when we use the data from relaxed muscle to train the model, but test it with data collected from tense muscle. Such difference could result from the stiffness variation caused by muscle contraction. To combat this problem, one solution is to consider such variation in the training phase. This can be simply done by using the response data collected from tense muscle to train the classifier. The result of "x-x" setting in the Figure 12 indicate such solution can perfectly alleviate this problem.

3) User Mobility: Another major confounding factor from user side is the user's mobility. As most of human mobility exhibit low frequency(less than 5 Hz), which is far away from the lowest frequency of our excitation(23 Hz), so we simply adopt a Butterworth bandpass filter to remove the inference of user mobility.

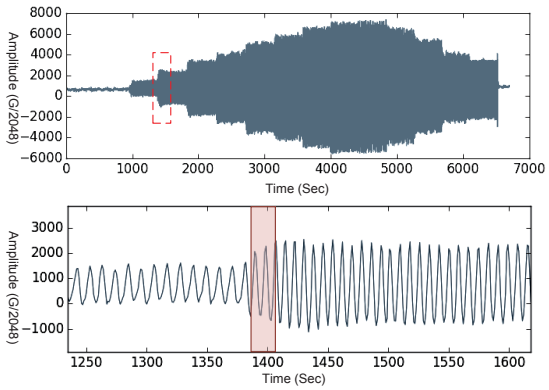

Fig. 16. Duration of transient state.

To evaluate the performance of VibID in mobile scenario, we ask volunteers to walk at normal pace during the data collection. Then, we compare the system performance under three different settings: (I). "s-s", in which we evaluate our system on data collected in static scenario via 10-fold cross validation; (II). "s-m", in which the classifier is trained by the static data, but tested with data collected from mobile scenario. (III). "x-x", which means the system is trained and tested with data from both static scenario and mobile scenario. According to Figure 13, we notice the precision and recall drop to 90.4% and 87.3% respectively in the "s-m" setting. This may be explained by the fact that there are still some interferences that cannot be filtered perfectly, such as the mobility inference from higher-order harmonics, or the ripple effect caused by FIR filter. However, such result is sufficient for our purpose and minor performance fluctuation is acceptable for our system.

C. Wearing Location

The key insight of VibID is the differences of the biological compositions of users' arm will cause the discrepancy in users' response data. However, in real application scenario, a major concern is that the wearing locations of our system can be quite different each time. For example, a user may normally wear VibID near the end of wrist at *Loc. 1* as shown in Figure 14, but in some cases, he may also wear the wristband at *Loc. 2*, *Loc. 3* or even *Loc. 4*. It is obvious that the underlying tissue composition of these locations are quite different. As a consequence, the response patterns of a single user change with wearing location, which eventually results in confusion in user identification.

To investigate the extent of this problem, we ask volunteers to wear our wristband at different locations as indicated in Figure 14, in which the distance between locations is one centimeter. For each wearing location, we collect 120 response data from 8 volunteers.

We start with a baseline test, in which we use the data collected from *Loc. 1* to train our classifier, then use the data collected from the other locations to test our model. Since we only use data from one wearing location to train the classifier, we term this experiment setting as "#loc $\leq$ 1 ". According to Figures 15, the system's performance significantly decreases as the testing location moving away from the training location. This is because the larger distance between the training location and testing location is, the more different the composition of underlying tissues will be.

A remedy is to consider the differences caused by wearing location in training phase. To validate this solution, we also conduct another experiment, in which we train a model with data collected from *Loc. 1* and *Loc. 2*, then test it with data from different locations. The result is labeled as "#loc $\leq$ 2 in Figure 15. We notice that this method can significantly increases the performance. Similar effect can be observed if we keep increasing the number of locations included in training phase. These result implies that we still ensure a relatively good performance by considering different wearing locations in training phase.

We acknowledge that, as there are many possible wearing locations which cannot be fully included in the training phase, this method can only alleviate the performance degradation. To completely solve the problem, one possible way is to quantify the changing trend in users' response data caused by the change of wearing locations. However, such analysis requires more volunteer participation and biological experiments, we leave it for future exploration.

D. Evaluation in Uncontrolled Scenario

To verify VibID's robustness to temporal changes of users' biological states and simulate the real application scenario of our system, we conduct a month-long evaluation in a uncontrolled scenario.

In this evaluation, we first ask volunteers to wear VibID wristband at different locations as indicated in Figure 14, and use the corresponding data to initialize our system. Then, instead of carefully controlling the confounding factors, we relax all the constraints and ask volunteers to use our system as she/he would like. Also, to investigate our system's robustness to user's biological changes over time, we intentionally collect the vibration responses of each user in several different weeks. For each user, we collect 120 response data in such uncontrolled setting and there are 960 responses (120×8 users) in total. Table III gives the basic biological information of each volunteer.

TABLE III
DETAILS OF HUMAN SUBJECTS

User No.	Age	Gender	Wrist Circumference	BMI
1	28	M	17.8	34.7
2	26	M	15.5	20.7
3	23	M	17.5	24.9
4	28	M	16.2	25.2
5	23	F	15.3	21.8
6	24	F	14.1	17.5
7	23	M	17.5	29.4
8	28	F	14.0	20.8

Then, we evaluate our system's performance under such setting by performing user identification with these data. Figure 17 shows the normalized confusion matrix, in which

	user 1	user 2	user 3	user 4	user 5	user 6	user 7	user 8
user 1	0.97	0	0	0.03	0	0	0	0
user 2	0	0.99	0.01	0	0	0	0	0
user 3	0	0.01	0.97	0	0	0	0.01	0.01
user 4	0	0	0	0.99	0.01	0	0	0
user 5	0.01	0	0	0.04	0.95	0	0	0
user 6	0	0	0	0	0	0.98	0.01	0.01
user 7	0	0.02	0.03	0	0	0	0.91	0.01
user 8	0	0	0.03	0	0	0	0.05	0.92

Fig. 17. Confusion matrix of user identification in uncontrolled scenario.

each item m_{ij} indicates the averaged percentage of the i-th user is identified as the j-th user. For example, $m_{55} = 0.95$ implies 95% of the response data from 5-th user is correctly classified, while $m_{54} = 0.04$ indicates 4% of her responses is misclassified as data from the 4-th user.

According to this matrix, we can observe the identification accuracy is quite high, the worst one is 91%. This result indicates that our system is robust to biological changes of users over time and can achieve a good performance in real application scenarios.

VI. Discussion

In this section, we discuss the limitation of VibID and the possible directions of further exploration.

A. Implementation Issue

We understand there are still some challenges need to be combated when implementing VibID on commercial off-the-shelf devices.

The first challenge derives from **the limitation of operating system**. As vibrators on existing wearable devices are mainly used for haptic feedback and notification, OS has placed many constraints on fine-grained control of its vibration patterns. For example, Android only provides an API to change the ON/OFF state of vibrator [23]. However, we envision that, with such available hardware and idea, wearable device and OS manufacturers can easily include such function into their future design.

Another concern rises from the **energy requirement of vibrator**: *Does such vibration-based system imply a high energy consumption?* There are some observations may help the justification for this issue: First, our system does not pose any strict requirement on the input voltage of vibrator. The frequency range of generated vibration mainly depends on the characteristics of vibrator, not the input voltage. Meanwhile, although our prototype adopts a vibrator with maximal 3.3V DC input (which is a common voltage standard for many IC board), any haptic vibrator available on wearable device should work as we only leverage the relative vibration amplitude, not the absolute value, in our identification model. Moreover, our system does not need frequent vibrations. It only needs to vibrate for 2 seconds at the moment when the user puts on our wristband. Such energy consumption is relatively minor comparing to the frequent notification or haptic feedback via vibration.

B. Usage Issues

As the function of VibID replies on vibration responses of users, it uses a short-term vibration as an excitation, a natural concern is **whether such vibration is obtrusive to users**. In fact, vibration is wildly adopted on many existing wearable devices as a method of notification and haptic feedback, *e.g.*, Fitbit Charge [1], Jawbone UP [24] and Apple watch [2]. Besides, as a user identification solution, VibID only needs to vibrate for 2 seconds at the moment when user puts on our system on his/her wrist. Such vibration is comparable to the vibration of notification and should be acceptable to users.

Apart from this, our system also pose some **requirements on how to use it**: we require the wristband is well-contacted with users' skin to ensure a good data quality. Also, to improve the system's robustness to wearing locations, we may need users to initialize our system with different wearing locations. However, such requirements are not demanding, many other existing identification systems also pose similar requirements. For instance, fingerprint reader requires a good contact between users' fingers and the sensor, while camera-based user identification needs to take users' portraits from different angles.

C. Future Exploration

To make our system more reliable and accurate, there are some directions worth to explore in the future:

- **Choice of excitation**. Due to the hardware limitation, our system leverage stepped sine sweeping as the excitation form. Further investigation on different excitation forms, *e.g.*, pseudo-random or fast sine chirp excitation [25], can help the improvement of identification accuracy.
- **Noise in more complicated scenarios**. Our prototype can only remove the noise caused by the users' movements, such as walking and texting. We can image there will be more noises in complicated scenarios, *e.g.*, riding on a bus. Future work will be focused on this area.
- **Long-term body variation**. Although we have investigated users' biological changes over weeks in our evaluation, our current prototype may not be able to handle the long-term body variation, *e.g.*, gaining or loosing weight in several months. One possible solution for such long-term change is to update our identification model over time. For example, each time a user is correctly recognized, we can update our model with his/her recent vibration response, and this process can be done periodically.

VII. Related Work

A. Modal analysis

The concept underlying our work resembles the modal analysis, which is a study of the dynamic properties of structures under vibration [25] and is widely used in the many engineer fields, such as: structure design [26–28], industrial manufacturing [29–31] and architecture damage detection [32–34]. There two different routes for modal analysis: the theoretical one starts with the dynamic properties of target structure, *i.e.*, the natural frequencies, damping and vibration mode shapes, and tries to analyze the response level of structure under different excitations. On the contrary, the experimental modal analysis estimates the dynamic properties by examining its vibration patterns. To obtain accuracy result, experimental modal analysis often requires strictly-controlled experiment settings and high quality data acquisition devices. Although inspired by the modal analysis, our system differs from it in two aspects: First, our system does not aim to exactly compute the dynamic properties from users' responses. Instead, we are only interested in leveraging the discrepancy in responses to identify users. Also, our system is not restricted in the strictly-controlled lab environment and we only needs low-cost devices/sensors.

B. User Identification on Wearable Devices

As user identification is a fundamental problem of the security and data privacy issues, extensive efforts have been devoted into the quest of a reliable and practical user identification solution for wearable devices.

In this field, many researches leverage the biometrics to identify users [4–6, 35]. The dedicated biometric devices, such as: capacitive touch screen [4], or bio-impedance sensor [5], are utilized to extract users' biometric as an identifier. For example, Vu *et al.* propose to use the charge variation caused by human finger touch on capacitive screen to detect the signature encoded in a specially-designed ring in [4]. However, the prevalence of these approaches is hindered by the requirement of dedicated devices. Instead of relying dedicate devices to measure the biometrics of users, some other works extract users' gaits from motion sensors, and leverage the gait patterns to distinguish users [6, 35]. Since gaits are only observable when user is moving, this solutions are limited to mobile scenario.

On the other hand, some researchers have investigated the possibility of performing user identification via usage behavior modeling. In [7], the authors use the data stream on mobile phone, *e.g.*, email, contact, cell tower ID or even the WiFi AP address, to model users' usage behavior. By comparing the usage patterns, the system can identify the users and detect anomaly usage. A similar idea is proposed in [8, 9], in which the authors build a user identification model with the user's touching behavior and reaction of device. As accurate user behavior modeling needs a large data set and requires high computation power, such approach does not fit well in the scenario of wearable devices.

Compared with these works, our system enables user identification with a vibration motor and accelerometer sensor, both of with are the existing low-cost devices available for most wearable devices. Besides, our system does not require any user intervention.

C. Vibration for Other Purpose

As a common physical phenomenon in our world, variation has been well-investigated and adopted in many areas. The authors in [36] proposed to a method to recover sound from silent videos by observing the environmental vibration caused by the sound, and they extent the idea to study the material prosperities in videos [37]. Meanwhile, Roy *et al.* [23] designed a system which enables communication between mobile phones by modulating information on mechanical vibrations, and the authors in [38] studied the privacy issues exposed by wireless vibrometry. As a complementation, our work proposes a method to leverage the vibration responses to identify users on wearable devices.

VIII. Conclusion

In this paper, we introduced VibID, a new user identification system for wearable devices through bio-vibrometry. The key idea is that the biological difference of users leads to a diversity in characteristics of users' body, and such difference is reflected in users' response to a mechanical vibration. Thus, we can leverage such discrepancy in vibration responses to distinguish users. By carefully design our system, we implement VibID with a vibrator motor and three-axis accelerometer, which are existing low-cost sensors available to most wearable devices. According to comprehensive experiments, we demonstrate our system is robust to various confounding factors and can achieve a good performance in small-scale scenarios.

Acknowledgments

We thank Tarek Abdelzaher for his feedback and guidance as our paper shepherd, and the anonymous reviewers for their invaluable comments. This research was supported in part by grants from 973 project 2013CB329006, RGC under the contracts CERG MHKUST609/13 and 622613, China NSFC under Grant 61502114.

References

[1] Fitbit charge. https://www.fitbit.com/charge.

[2] Apple watch. http://www.apple.com/watch/.

[3] Google glucose lens. http://time.com/3758763/google-smart-contact-lens/.

[4] T. Vu and *et al.*, "Distinguishing users with capacitive touch communication," in *Proceedings of the 18th Annual International Conference on Mobile Computing and Networking*, ser. Mobicom '12. ACM, 2012, pp. 197–208.

[5] C. Cornelius, R. Peterson, J. Skinner, R. Halter, and D. Kotz, "A wearable system that knows who wears it," in *Proceedings of the 12th annual international conference*

on Mobile systems, applications, and services. ACM, 2014, pp. 55–67.

[6] Y. Ren and *et al.*, "Smartphone based user verification leveraging gait recognition for mobile healthcare systems," in *Sensor, Mesh and Ad Hoc Communications and Networks (SECON)*, 2013, pp. 149–157.

[7] S. Buthpitiya, A. K. Dey, and M. Griss, "Soft authentication with low-cost signatures," in *Pervasive Computing and Communications (PerCom), 2014 IEEE International Conference on*. IEEE, 2014, pp. 172–180.

[8] C. Bo and *et al.*, "Silentsense: silent user identification via touch and movement behavioral biometrics," in *Proceedings of the 19th annual international conference on Mobile computing & networking*. ACM, 2013, pp. 187–190.

[9] S. M. Kolly, R. Wattenhofer, and S. Welten, "A personal touch: Recognizing users based on touch screen behavior," ser. PhoneSense '12. ACM, 2012.

[10] S. S. Rao and F. F. Yap, *Mechanical vibrations*. Addison-Wesley Reading, 1995, vol. 4.

[11] W. E. Siri, "The gross composition of the body," *Adv Biol Med Phys*, vol. 4, no. 239-279, p. 513, 1956.

[12] Precsion hatpic vibration motor model 306-109. [Online]. Available: https://catalog.precisionmicrodrives.com/order-parts/product/306-109-6mm-vibration-motor-12mm-type

[13] Invensense mpu-6050. [Online]. Available: http://www.invensense.com/products/motion-tracking/6-axis/mpu-6050

[14] S. Adewusi and *et al.*, "Vibration transmissibility characteristics of the human hand–arm system under different postures, hand forces and excitation levels," *Journal of sound and vibration*, vol. 329, no. 14, pp. 2953–2971, 2010.

[15] S. Adewusi, M. Thomas, V. Vu, and W. Li, "Modal parameters of the human hand-arm using finite element and operational modal analysis," *Mechanics & Industry*, vol. 15, no. 6, pp. 541–549, 2014.

[16] M. Barr, "Pulse width modulation," *Embedded Systems Programming*, vol. 14, no. 10, pp. 103–104, 2001.

[17] J. R. Kwapisz, G. M. Weiss, and S. A. Moore, "Activity recognition using cell phone accelerometers," *ACM SigKDD Explorations Newsletter*, vol. 12, no. 2, pp. 74–82, 2011.

[18] L. Zhang and *et al.*, "Accelword: Energy efficient hotword detection through accelerometer," in *Proceedings of the 13th Annual International Conference on Mobile Systems, Applications, and Services*. ACM, 2015, pp. 301–315.

[19] L. R. Rabiner and B. Gold, "Theory and application of digital signal processing," *Englewood Cliffs, NJ, Prentice-Hall, Inc., 1975. 777 p.*, vol. 1, 1975.

[20] L. Breiman, "Random forests," *Machine Learning*, 2001.

[21] F. Pedregosa and *et al.*, "Scikit-learn: Machine learning in Python," *Journal of Machine Learning Research*, vol. 12, pp. 2825–2830, 2011.

[22] C. M. Bishop, *Pattern recognition and machine learning*. springer, 2006.

[23] N. Roy, M. Gowda, and R. R. Choudhury, "Ripple: Communicating through physical vibration," in *Proceedings of the 12th USENIX Conference on Networked Systems Design and Implementation*, ser. NSDI'15, 2015, pp. 265–278.

[24] Jawbone. https://jawbone.com/.

[25] D. J. Ewins, *Modal testing: theory and practice*. Research studies press Letchworth, 1995, vol. 6.

[26] M. Priestley, G. Calvi, and M. Kowalsky, "Direct displacement-based seismic design of structures," in *2007 NZSEE Conference*, 2007.

[27] Z. Ping and *et al.*, "The modal analysis and optimum structure design of passenger car body," *Automobile Technology*, vol. 4, p. 001, 2006.

[28] W.-X. Ren, T. Zhao, and I. E. Harik, "Experimental and analytical modal analysis of steel arch bridge," *Journal of Structural Engineering*, vol. 130, no. 7, pp. 1022–1031, 2004.

[29] B. Gao, G. Morison, and P. Kundur, "Voltage stability evaluation using modal analysis," *Power Systems, IEEE Transactions on*, vol. 7, no. 4, pp. 1529–1542, 1992.

[30] A. Wexler, "Solution of waveguide discontinuities by modal analysis," *Microwave Theory and Techniques, IEEE Transactions on*, vol. 15, no. 9, pp. 508–517, 1967.

[31] K. D. Marshall, "Modal analysis of a violin," *The Journal of the Acoustical Society of America*, vol. 77, no. 2, pp. 695–709, 1985.

[32] A. Pandey, M. Biswas, and M. Samman, "Damage detection from changes in curvature mode shapes," *Journal of sound and vibration*, vol. 145, no. 2, pp. 321–332, 1991.

[33] G. Hearn and R. B. Testa, "Modal analysis for damage detection in structures," *Journal of Structural Engineering*, vol. 117, no. 10, pp. 3042–3063, 1991.

[34] P. Hajela and F. Soeiro, "Structural damage detection based on static and modal analysis," *AIAA journal*, vol. 28, no. 6, pp. 1110–1115, 1990.

[35] T. Teixeira and *et al.*, "Pem-id: Identifying people by gait-matching using cameras and wearable accelerometers," in *Distributed Smart Cameras, 2009. ICDSC 2009. Third ACM/IEEE International Conference on*. IEEE, 2009, pp. 1–8.

[36] A. Davis and *et al.*, "The visual microphone: Passive recovery of sound from video," *ACM Transactions on Graphics (Proc. SIGGRAPH)*, vol. 33, no. 4, pp. 79:1–79:10, 2014.

[37] A. Davis, K. L. Bouman, J. G. Chen, M. Rubinstein, F. Durand, and W. T. Freeman, "Visual vibrometry: Estimating material properties from small motions in video," in *Computer Vision and Pattern Recognition (CVPR), 2015 IEEE Conference on*. IEEE, 2015, pp. 5335–5343.

[38] T. Wei and *et al.*, "Acoustic eavesdropping through wireless vibrometry," in *Proceedings of the 21st Annual International Conference on Mobile Computing and Networking*. ACM, 2015, pp. 130–141.